

Geological Survey
of Canada



Current Research 2000-E10

Electrical conductivity mechanism of sericitic schist samples from Giant and Con mine areas, Yellowknife mining district, Northwest Territories

S. Connell, P. Hunt, and T.J. Katsube

2000



Natural Resources
Canada

Ressources naturelles
Canada

Canada

©Her Majesty the Queen in Right of Canada, 2000
Catalogue No. M44-2000/E10E-IN
ISBN 0-660-18214-9

Available in Canada from the
Geological Survey of Canada Bookstore website at:
<http://www.nrcan.gc.ca/gsc/bookstore> (Toll-free: 1-888-252-4301)

A copy of this publication is also available for reference by depository
libraries across Canada through access to the Depository Services Program's
website at <http://dsp-psd.pwgsc.gc.ca>

Price subject to change without notice

All requests for permission to reproduce this work, in whole or in part, for purposes of commercial use, resale or redistribution shall be addressed to: Geoscience Information Division, Room 200, 601 Booth Street, Ottawa, Ontario K1A 0E8.

Authors' address

S. Connell (sconnell@nrcan.gc.ca)
P. Hunt (phunt@nrcan.gc.ca)
T.J. Katsube (jkatsube@nrcan.gc.ca)
Mineral Resources Division
Geological Survey of Canada
601 Booth Street
Ottawa, Ontario K1A 0E8

Electrical conductivity mechanism of sericitic schist samples from Giant and Con mine areas, Yellowknife mining district, Northwest Territories¹

S. Connell, P. Hunt, and T.J. Katsube
Mineral Resources Division, Ottawa

Connell, S., Hunt, P., and Katsube, T.J., 2000: Electrical conductivity mechanism of sericitic schist samples from Giant and Con mine areas, Yellowknife mining district, Northwest Territories; Geological Survey of Canada, Current Research 2000-E10; 7 p. (online; <http://www.nrcan.gc.ca/gsc/bookstore>)

Abstract: Detailed textural examination using scanning electron microscope analysis was performed on six sericitic and chloritic-sericite schist samples in a preliminary study designed to determine the electrical resistivity characteristics of alteration zones that accompany gold-bearing quartz veins in the Yellowknife mining district. The purpose was to obtain information required to help develop efficient exploration strategies.

Results indicate that a multilayer electrically anisotropic model consisting of thin alternating resistive and conductive layers applies to five of the six samples studied. The conductive layers are characterized by platy, fine-grained micaceous material, resulting in significant but moderately low electrical resistivity values (360–6600 $\Omega\cdot\text{m}$) in the direction parallel to foliation, likely due to moderately good pore-fluid connectivity. Sulphide minerals have had little to no effect on these resistivities. The resistive layers consist of quartz and ankerite. The low electrical resistivity characteristics of the sixth sample are likely determined by a well developed fracture system.

Résumé : Six échantillons de séricitoschiste et de séricitoschiste chloritique ont été soumis à un examen détaillé de la texture par microscopie électronique à balayage dans le cadre d'une étude préliminaire visant à déterminer les caractéristiques de résistivité électrique des zones d'altération accompagnant les filons de quartz aurifère dans le district minier de Yellowknife. L'étude avait pour objet d'obtenir l'information nécessaire à l'élaboration de stratégies d'exploration efficaces.

Les résultats indiquent qu'un modèle multicouche anisotrope du point de vue électrique et consistant en minces couches résistantes et conductrices alternées convient pour cinq des six échantillons étudiés. Les couches conductrices sont caractérisées par un matériau micacé aplati à grain fin, ce qui leur confère des valeurs de la résistivité électrique significatives mais relativement faibles (de 360 à 6 600 $\Omega\cdot\text{m}$) dans la direction parallèle à la schistosité, vraisemblablement en raison d'une modérément bonne connectivité des fluides interstitiels. Les sulfures n'ont eu que peu ou pas d'effet sur ces résistivités. Les couches résistantes consistent en quartz et en ankerite. La faible résistivité électrique du sixième échantillon dépend vraisemblablement d'un réseau de fractures bien développé.

¹ Contribution to the 1999-2003 Yellowknife, Canada-Northwest Territories Exploration Science and Technology (EXTECH III) Initiative

INTRODUCTION

Detailed textural examination using scanning electron microscope (SEM) analysis was carried out on four sericitic schist and chloritic sericite schist samples, represented by six subsamples, from the Con and Giant mines in the Yellowknife mining district. This was a preliminary study designed to determine the electrical conductivity mechanisms of the mineralized sericitic schist from alteration zones that parallel the gold-bearing quartz veins in the Yellowknife mining district. Electrical resistivity measurements made on these mineralized rocks (Scromeda et al., 2000) indicate that they display moderate anisotropic characteristics (3:1 to 14:1), with the high and low resistivities in the ranges of 300–600 $\Omega\cdot\text{m}$ and 2400–7500 $\Omega\cdot\text{m}$ in the directions parallel and perpendicular to foliation, respectively. Although these values are unusually low for typical crystalline rocks (Katsube and Mareschal, 1993), they are at the high end for mineralized rocks (e.g. Katsube et al., 1997). It is therefore necessary to understand the electrical mechanisms that determine the electrical resistivity characteristics of these rocks in order to facilitate development of efficient geophysical exploration strategies. In this paper, description of the methods used for investigation are followed by detailed descriptions of the rock texture and discussions regarding implications for electrical conductivity mechanisms.

METHOD OF INVESTIGATION

The four samples, highlighted in this study, were selected from a set of ten samples which had previously been used for 3-D electrical resistivity measurements (Scromeda et al., 2000; Connell et al., 2000). Two of the samples were each divided in to two subsamples in order to isolate particular areas of interest (e.g. veins, mineralized sections) resulting in these four samples being represented by six subsamples. Information on sample depth and lithology is listed in

Table 1. Six subsamples (MYC-1, MYC-2A, MYC-2B, MYG-11A, MYG-11B, and MYG-13) were prepared for SEM analysis.

The subsamples used for the electrical measurements were previously cut into rectangular-shaped blocks (Scromeda et al., 2000), with one side parallel to foliation and the other two sides cut perpendicular to foliation. First, a detailed visual examination was performed on these subsamples and key features recorded, as shown in the block diagrams in Figures 1–4. Then, relevant surfaces were polished and prepared for the SEM analysis. This analysis included examination of sample mineralogy, texture, and fabric of the sulphide and other mineral grains that influence the flow of electrical currents through the rock.

A Leica/Cambridge S-360 scanning electron microscope (SEM) with an Oxford/Link eXL-II energy dispersive X-ray analyser was used for this analysis. Operating conditions for the SEM were generally 20 kV accelerating voltage at a 25 mm working distance. Backscattered electron images (BSI) were produced as a result. A detailed description of SEM methods and procedures can be found elsewhere (Reed, 1997).

The electrical conductivity model of rocks consisting of thin (0.5–10 mm) multilayers of high and low electrical resistivity (Katsube et al., 1997; Connell et al., 1999) were used in this analysis. High electrical resistivity layers typically consist of tightly connected electrically insulating minerals (e.g. quartz, feldspar, calcite) and result in high bulk electrical resistivities of the sample in the direction parallel to the layers. Low electrical resistivity layers typically consist of either thin tightly interconnected electronically conductive minerals (e.g. pyrite, chalcopyrite, magnetite, galena, graphite) or of fine-grained minerals assumed to contain reasonable to considerable amounts of pore space which result in low bulk electrical resistivities in the direction parallel to the layers. For the fine-grained layers, it is generally assumed that pore-fluid connectivity tends to allow the electrical current to flow parallel to the layers.

Table 1. Rock descriptions, depths and results of the electrical resistivity measurements (Scromeda et al., this volume) for four sericitic samples represented by six subsamples collected from the Con and Giant mines (Yellowknife, Northwest Territories).

Sample number	Stope	Lithology	Sulphide content (%)	ϕ_E (%)	Mean ρ_r ($10^3 \Omega\cdot\text{m}$)			Anisotropy (λ)
					α	β	γ	
<i>Con mine</i>								
MYC-1	3148R	SS	< 2 %	1.16	5.90 ± 2.4	0.98 ± 0.32	0.60 ± 0.16	10:1
MYC-2A	3148R	CSS	2 %	0.80	1.56 ± 0.36	3.61 ± 0.9	5.38 ± 0.23	3:1
MYC-2B			trace		7.51 ± 0.74	4.45 ± 0.98	1.96 ± 0.32	4:1
<i>Giant mine</i>								
MYG-11A	370	SS	5–7 %	1.97	5.08 ± 0.09	0.36 ± 0.0	0.62 ± 0.01	14:1
MYG-11B			2 %	2.86	1.62 ± 0.05	2.97 ± 0.05	6.61 ± 0.31	4:1
MYG-13	370	SS	2–3 %	1.46	2.40 ± 0.26	1.25 ± 0.15	0.58 ± 0.02	4:1

ϕ_E = Effective porosity (%)
 ρ_r = Mean bulk electrical resistivity after 24 and 48 hours saturation
 CSS = Chlorite-sericite schist
 SS = Sericite schist

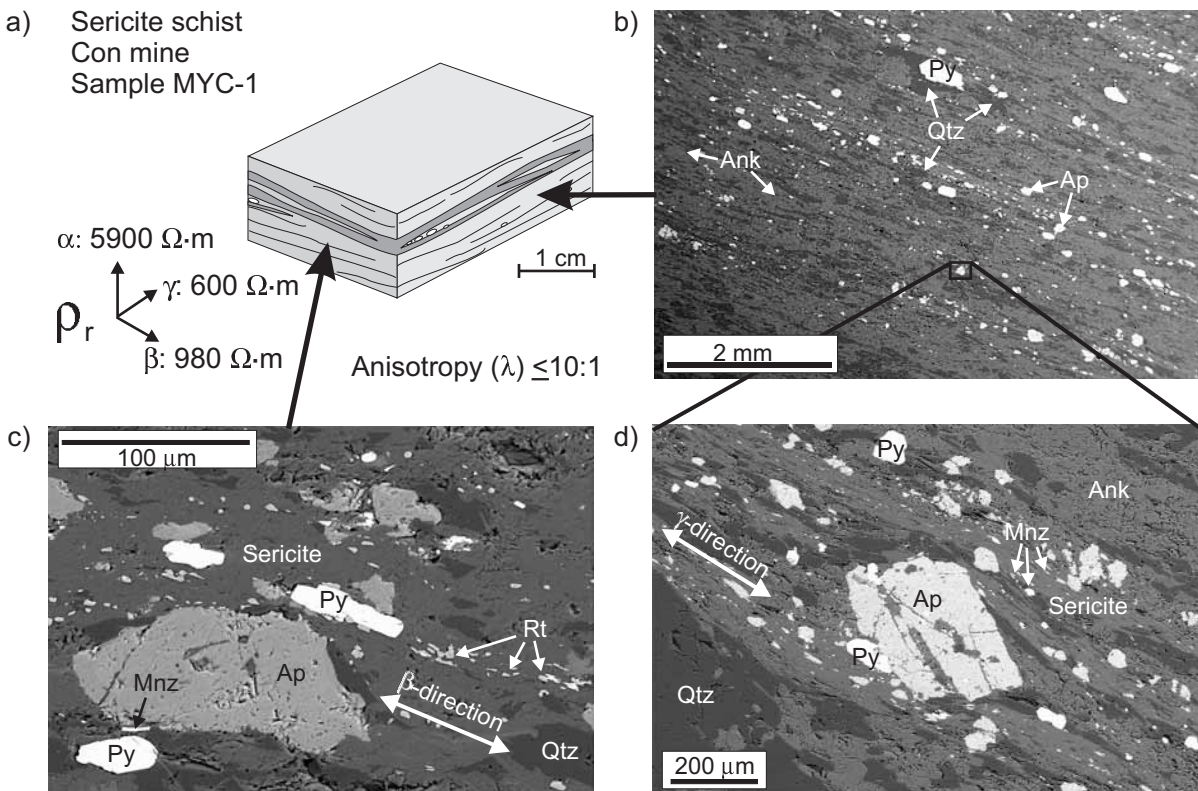


Figure 1. Schematic presentation of a sericite schist sample MYC-1 (Con mine) represented by **a)** a block diagram with sketches of the rock texture and 3-D electrical resistivity (ρ_r) and anisotropy (λ) values shown below. Scanning electron microscope (SEM) images are also displayed for surfaces perpendicular to the **b)** and **c)** β -axis (side of sample), and **d)** γ -axis (side of sample) of the sample block. The SEM images (backscattered image, BSI) show the orientation and distribution of the pyrite (Py), apatite (Ap), monazite (Mnz), rutile (Rt), sericite (lighter grey mineral), ankerite (Ank), and quartz (Qtz: dark grey).

ANALYTICAL RESULTS AND INTERPRETATION

A schematic presentation of a sample from the sericite schist sample MYC-1 (Con mine) is displayed in Figure 1a. The directions of electrical resistivities (ρ_r) are shown below the block diagram with 600–980 $\Omega \cdot m$ and 5900 $\Omega \cdot m$ in the directions parallel and perpendicular to foliation, respectively. The electrical resistivity anisotropy (λ) for this sample is less than 10:1. The mineralogy includes ankerite, quartz, sericite, rutile, pyrite, apatite, galena, and monazite, which were all identified under the SEM (Fig. 1b, c, d). Not all minerals identified under the SEM are shown in these images. The rock texture and sulphide grain distribution are shown in the SEM image in Figure 1b, with more details shown in the images in Figures 1c and 1d. There is a general preferential alignment of the platy mineral grains parallel to foliation, but a poor connectivity between the sulphide grains. The lower resistivity values are associated with the preferential alignment of these platy minerals. The parallel alignment of platy minerals in the β - and γ -directions and the possible good pore-fluid connectivity between intergranular pores, likely constitutes the main

electrical conductivity mechanism that produces the lower ρ_r values (600–980 $\Omega \cdot m$) in the directions parallel to foliation. In the α -direction (perpendicular to foliation), the quartz- and ankerite-rich layers are likely forming electrically insulating layers that interrupt the flow of the electrical current in that direction, thereby creating the increased ρ_r values (5900 $\Omega \cdot m$) in that direction. The orientation of the foliation in these SEM images may appear different from that in the sketch due to the position of the sample in the sample holder under the SEM (e.g. Fig. 1d).

Schematic presentations of chlorite-sericite schist subsamples MYC-2A and MYC-2B are displayed in Figure 2a. The ρ_r values in the three directions for the two subsamples are displayed below each of their two block diagrams. SEM images of the top and side sections of MYC-2A are displayed in Figures 2b and 2c, and the top section of MYC-2B is displayed in Figure 2d. Quartz, plagioclase, ankerite, sericite, pyrite, apatite, chlorite, rutile, monazite, and zircon have been identified under the SEM for both samples, except pyrite which was not identified in MYC-2B. MYC-2A represents a folded portion of the chlorite-sericite schist containing a vein, and MYC-2B represents the same

type of rock without the vein. The γ -direction and α -direction are perpendicular to foliation for these two subsamples, respectively. For MYC-2A, ρ_r values measured parallel (α - and β -directions) and perpendicular (γ -direction) to foliation are 1560–3610 $\Omega\cdot m$ and 5380 $\Omega\cdot m$, respectively, with an λ value of 3:1. For MYC-2B, ρ_r values measured parallel (β - and γ -direction) and perpendicular (α -direction) to foliation are 4450–1960 $\Omega\cdot m$ and 7510 $\Omega\cdot m$, respectively, with an λ value

of 4:1. The sulphide grains are generally euhedral to subhedral in shape for MYC-2A, and the fold is defined by a layer of undeformed pyrite (some connection between grains) and apatite grains shown in the SEM images (Fig. 2b, 2c). The lower ρ_r values (4450–1960 $\Omega\cdot m$) in the β - and γ -directions of MYC-2B are likely a result of the platy minerals (chlorite and sericite seen in Fig. 2d) aligned parallel to foliation and not due to sulphide minerals. This is because there were no sulphide minerals identified under the SEM. This is

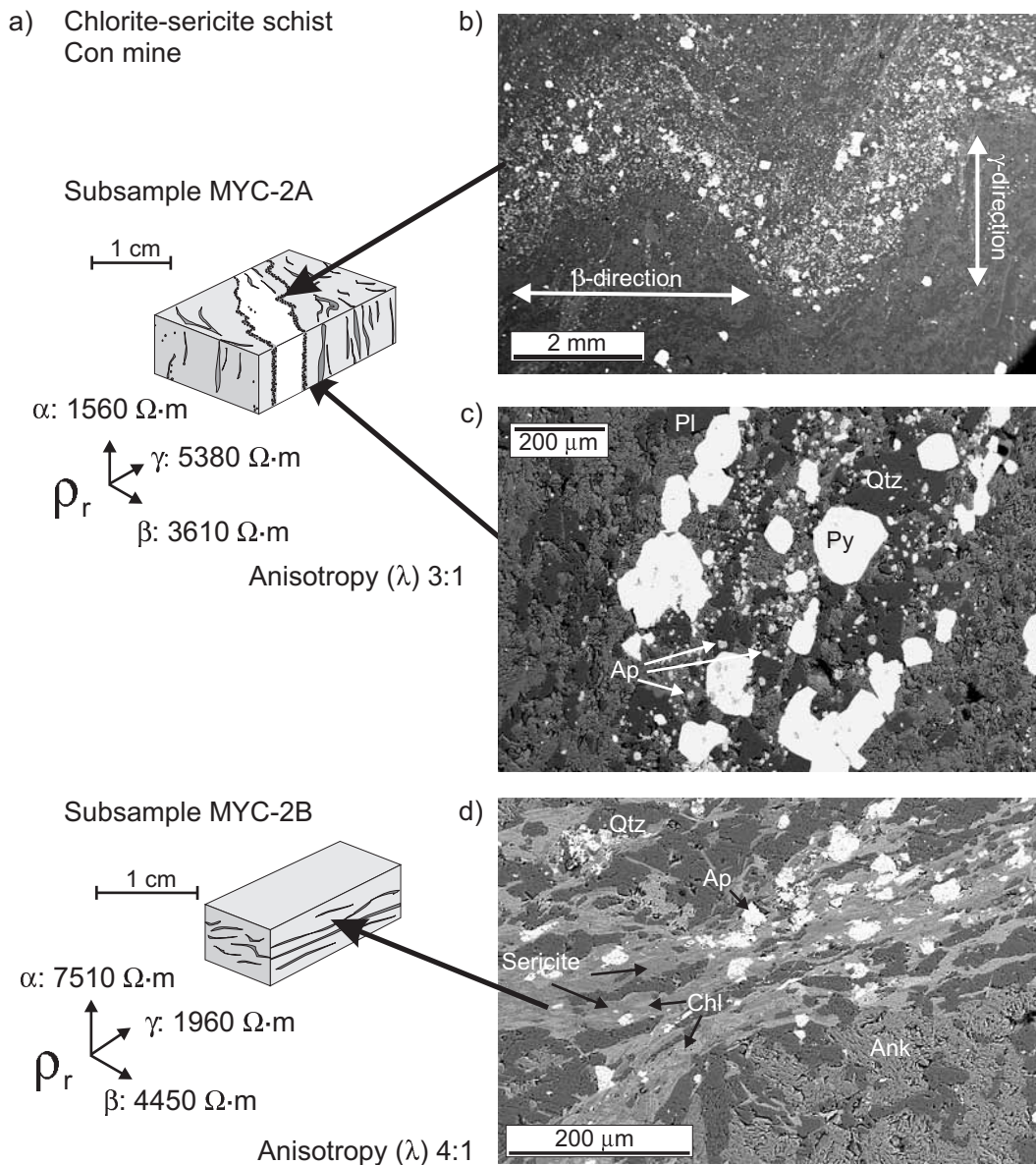


Figure 2. Schematic presentations of chlorite-sericite schist subsamples MYC-2A and MYC-2B (Con mine) represented by a) block diagrams with sketches of the rock texture and 3-D ρ_r and λ values shown below. Scanning electron microscope images displayed for surfaces perpendicular to the b) α -axis (top side of sample sketch) and c) β -axis (side of sample sketch) for subsample MYC-2A and d) β -axis (side of sample sketch) for subsample MYC-2B. The SEM images show the fold defined by pyrite (Py) and apatite (Ap) (Fig. 2b, c) and distribution and orientation of chlorite (Chl: light grey), sericite (light grey), ankerite (Ank), and quartz (Qtz: dark grey).

supported by the fact that the high sulphide concentration in the folded vein of MYC-2A (Fig. 2b) does not appear to have influenced the ρ_r values (1560–3610 $\Omega\cdot\text{m}$) in the directions parallel to foliation (α - and β -directions).

Schematic presentations for sericite schist subsamples MYG-11A and MYG-11B are displayed in Figure 3a. The directions of the ρ_r values are shown below each block diagram. The SEM images are displayed on the right-hand side

of the diagram. The mineralogy identified by SEM includes ankerite, quartz, chlorite, sericite, pyrite, arsenopyrite, rutile, and stibnite. Subsample MYG-11A has ρ_r values of 360–620 $\Omega\cdot\text{m}$ and 5080 $\Omega\cdot\text{m}$ parallel and perpendicular to foliation, respectively, and an λ value of 14:1. Subsample MYG-11B has ρ_r values of 1620–2970 $\Omega\cdot\text{m}$ and 6610 $\Omega\cdot\text{m}$ parallel and perpendicular to foliation, respectively, and an λ value of 4:1. Subsample MYG-11A shows a more distinct

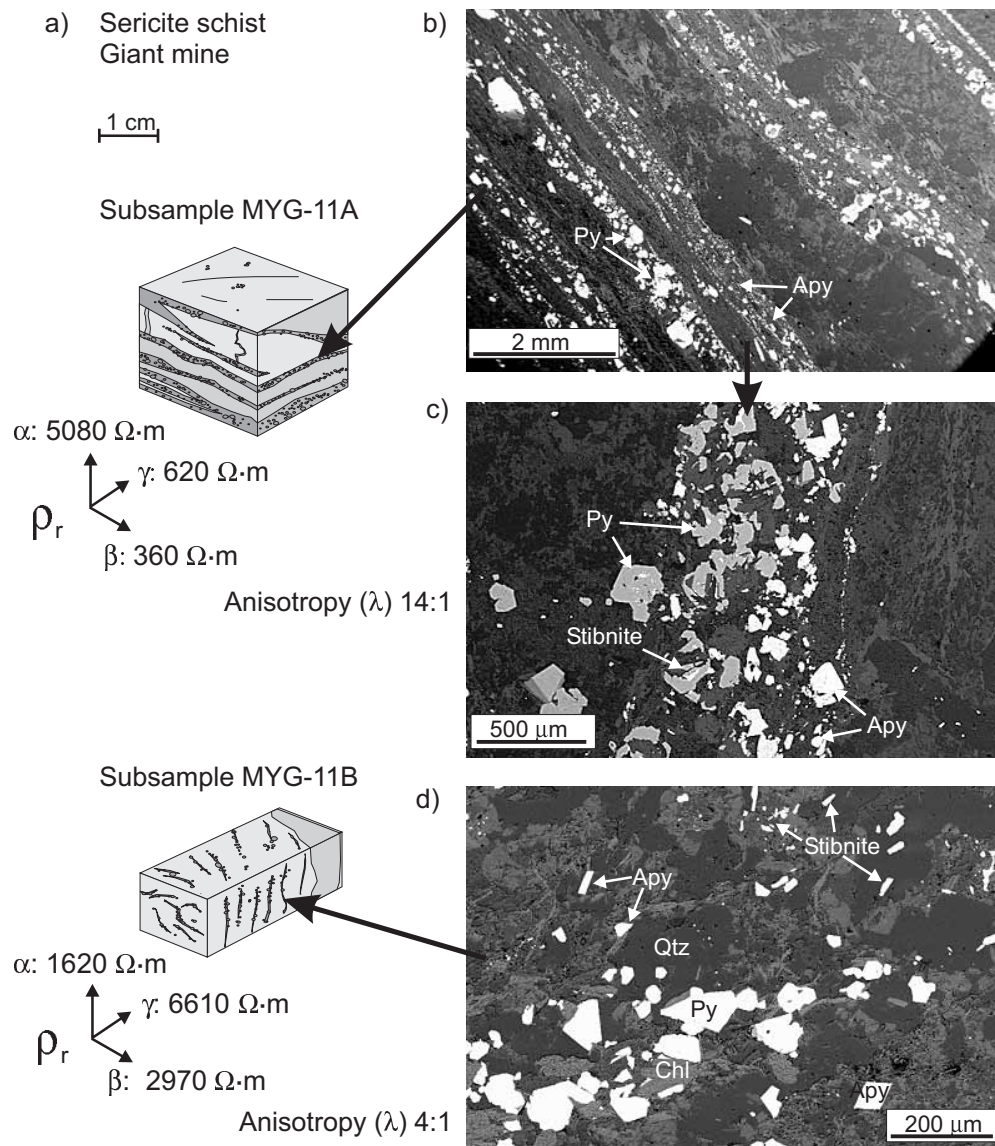


Figure 3. Schematic presentations of sericite schist subsamples MYG-11A and MYG-11B (Giant mine) represented by a) block diagrams with sketches of the rock texture and 3-D ρ_r and λ values shown below. Scanning electron microscope images displayed for surfaces perpendicular to the β -axis (side of sample sketch) b) and an enlargement of the same surface c) of subsample MYG-11A and d) perpendicular to β -axis (side of sample sketch) for subsample MYG-11B. The SEM images (backscattered image, BSI) show the foliation, distribution of sulphide and other minerals identified (pyrite (Py), arsenopyrite (Apy), chlorite (Chl: light grey), stibnite, and quartz (Qtz: dark grey)).

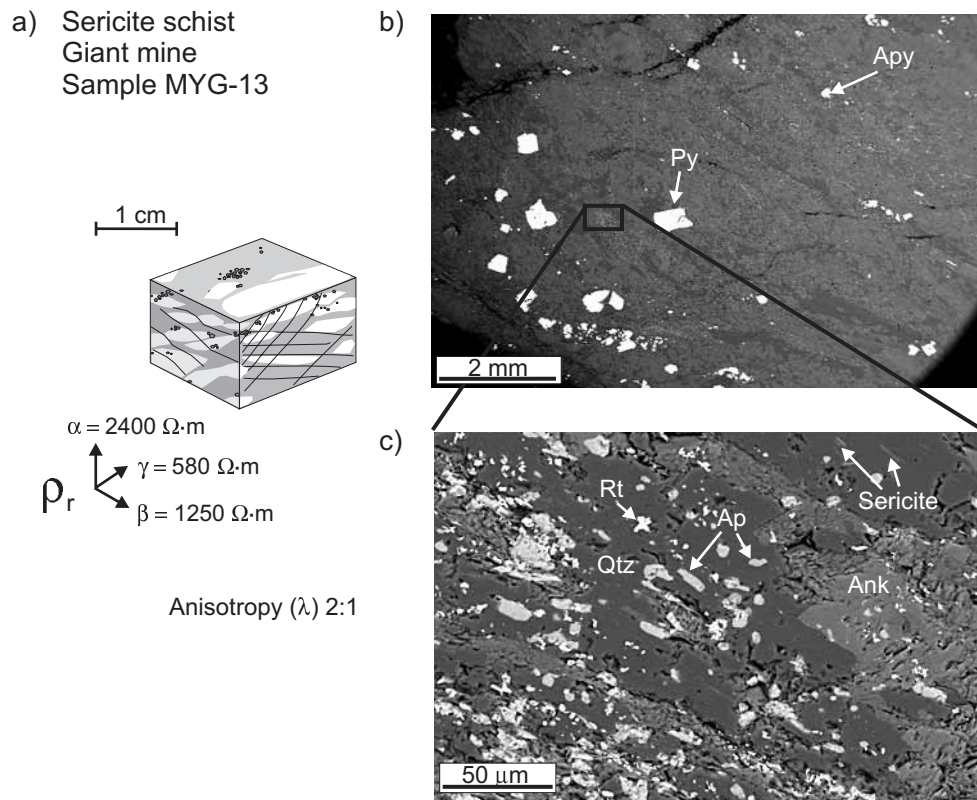


Figure 4. Schematic presentation of a sericite schist sample MYG-13 (Giant mine) represented by **a)** a block diagram with sketches of the rock texture and 3-D ρ_r and λ values shown below. Scanning electron microscope images displayed **b)** and **c)** for surfaces perpendicular to the β -axis (side of sample sketch). The SEM images (backscattered image, BSI) show the distribution of sulphides and minerals identified (pyrite (Py), arsenopyrite (Apy), apatite (Ap), rutile (Rt), ankerite (Ank), sericite, and quartz (Qtz)).

foliation and higher sulphide content compared to MYG-11B (and all other samples), which probably explains its lower ρ_r values in the direction parallel to foliation and its higher λ value. The layering of the sulphide minerals in subsample MYG-11A is shown in Figures 3b and 3c. There is preferential separation of sulphide from nonsulphide minerals, resulting in distinct pyrite and arsenopyrite layers. A view perpendicular to foliation for subsample MYG-11B (Fig. 3d), show that the concentration of the sulphide grains is considerably lower than in MYG-11A. The reason for the low ρ_r values in the direction parallel to foliation for MYG-11A are likely the thin (1–2 mm) layers with increased sulphide concentration. The reason for the high ρ_r values in the direction perpendicular to foliation are the layers of quartz and ankerite forming the electrically insulating layers.

A schematic presentation of sample MYG-13 is displayed in Figure 4a. The electrical resistivities for the three directions are shown below the block diagram. The ρ_r values for the α -, β - and γ -directions are 2400 $\Omega \cdot m$, 1250 $\Omega \cdot m$ and 580 $\Omega \cdot m$, respectively. Ankerite, quartz, rutile, sericite, pyrite, and arsenopyrite are identified by SEM. Although

there is a less well developed foliation than in other samples, the sample is highly fractured, thereby making an accurate characterization of it difficult.

DISCUSSION AND CONCLUSIONS

In previous studies of non-gold-bearing rocks where sulphide concentrations resulted from folding (e.g. Jones et al., 1997; Katsube et al., 1997), the folding had caused deformation of sulphide grains, sulphide concentrations in fold hinges, and well interconnected sulphide layers which resulted in very low ρ_r values in directions parallel to bedding. In this study, the ρ_r values in the direction parallel to foliation (1560–3610 $\Omega \cdot m$) for chlorite-sericite schist sample MYC-2A are considerably higher than many such values in these previous studies (<10 $\Omega \cdot m$), likely due to the poor connectivity between sulphide grains.

Sample MYG-13 is highly fractured, thereby making the determination of the source of its electrical anisotropy difficult. Formation-factor measurements would be useful in determining whether the anisotropy is a result of the less well

developed foliation or the fractures which are generally oriented parallel to each of the β - and γ -directions. This type of measurement would also indicate whether the increased electrical conductivity in sericite schist sample MYC-1 is only a result of good pore-fluid connectivity in that direction or whether there is some contribution from the sulphide grains, or both. Applications of such formation-factor measurements can be found in the literature (Katsube and Mareschal, 1993; Katsube and Salisbury, 1994).

This study indicates that the electrical anisotropy (λ) for these four sericitic schist samples, represented by six subsamples, are in the range of 2:1 to 14:1 and the electrical resistivity (ρ_r) values in the direction parallel and perpendicular to foliation are in the ranges of 360–4450 $\Omega\cdot\text{m}$ and 2400–7510 $\Omega\cdot\text{m}$ (Table 1, Fig. 1–4), respectively. The mineralogy varies little between these schist samples, primarily quartz, sericite, ankerite, chlorite, rutile, and pyrite being identified in varying amounts. Arsenopyrite and stibnite are also present in the Giant mine samples. The sulphide content, which is variable, does not appear to control the electrical conductivity. For example, there are significantly more sulphide minerals in sample MYG-11, and yet its ρ_r values (360–6610 $\Omega\cdot\text{m}$) are similar to those (600–5900 $\Omega\cdot\text{m}$) of MYC-1, which has the lowest sulphide content.

The results of this study suggests that the multilayer electrical conductivity model (Katsube et al., 1997; Connell et al., 1999) applies to all of these samples (MYC-1, MYC-2A, MYC-2B, MYG-11A, MYG-11B), except MYG-13 in which the anisotropic electrical resistivity characteristics are more likely determined by the fracture system than the less well developed foliation. The low resistivity layers for the other three samples (five subsamples) are characterized by platy fine-grained material (primarily sericite), resulting in the moderately low electrical resistivity values (360–6600 $\Omega\cdot\text{m}$) in the direction parallel to foliation. This is likely due to moderately good pore-fluid connectivity. Sulphide minerals have had little to no effect on the electrical resistivity of these layers, for this set of samples. Quartz and ankerite layers oriented parallel to foliation form electrically insulating layers that interrupt the flow of electrical current, and result in the high electrical resistivities (2400–7500 $\Omega\cdot\text{m}$) in the direction parallel to foliation.

ACKNOWLEDGMENTS

The authors are grateful for the critical review of this paper and for the useful suggestions by John Kerswill (Geological Survey of Canada). This work has been supported by the EXTECH-III (Exploration and Technology) Project which was initiated in 1999 in the Yellowknife mining district, Northwest Territories.

REFERENCES

- Connell, S., Katsube, T.J., Hunt, P.A., and Walker, D.**
1999: Textural characteristics of rocks that display significant electrical anisotropy; *in* Current Research 1999-D; Geological Survey of Canada, p. 9–15.
- Connell, S., Scromeda, N., Katsube, T.J., and Mwenifumbo, J.**
2000: Electrical resistivity characteristics of mineralized and unmineralized rocks from Giant and Con mine areas, Northwest Territories; Geological Survey of Canada, Current Research 2000-E9; (online; <http://www.nrcan.gc.ca/gsc/bookstore>).
- Jones, A.G., Katsube, T.J., and Schwann, P.**
1997: The longest conductivity anomaly in the world explained; Sulphides in fold hinges causing very high electrical anisotropy; *Journal of Geomagnetism and Geoelectricity*, v. 49, p. 1619–1629.
- Katsube, T.J. and Mareschal, M.**
1993: Petrophysical model of deep electrical conductors; graphite lining as a source and its disconnection due to uplift; *Journal of Geophysical Research*, v. 98, no. B5, p. 8019–8030.
- Katsube, T.J. and Salisbury, M.**
1994: Implications of laboratory electrical measurements on interpretation of EM-surveys and origin of the Sudbury Structure; *Geophysical Research Letters (GRL)*, v. 21, p. 947–950.
- Katsube, T.J., Scromeda, N., Goodfellow, W.D., and Best, M.E.**
1997: Electrical characteristics of mineralized and nonmineralized rocks at the Brunswick No. 12 deposit, Bathurst mining camp, New Brunswick; *in* Current Research 1997-E; Geological Survey of Canada, p. 97–107.
- Reed, S.J.B.**
1997: *Electron Microprobe Analysis*; Cambridge University Press, Cambridge, United Kingdom, 346 p. (second edition).
- Scromeda, N., Connell, S., and Katsube, T.J.**
2000: Petrophysical properties of mineralized and nonmineralized rocks from Giant and Con mine areas, Northwest Territories; Geological Survey of Canada, Current Research 2000-E8; (online; <http://www.nrcan.gc.ca/gsc/bookstore>).

Geological Survey of Canada Project 870057